Nonstoichiometry and defect structure of spinel $LiMn_2O_{4-\delta}$

Jun Sugiyama [a,*], Taroh Atsumi [b,1], Tatsumi Hioki [a], Shoji Noda [a], Naoki Kamegashira [b]

[a] Toyota Central Research and Development Laboratories, Inc., Yokomichi 41-1, Nagakute, Aichi 480-11, Japan
[b] Department of Materials Science, Toyohashi University of Technology, Tempaku-cho, Toyohashi, Aichi 411, Japan

Abstract

The oxygen nonstoichiometry, δ, has been determined for a spinel $LiMn_2O_{4-\delta}$ sample as a function of oxygen partial pressure pO_2 in the 873–1123 K temperature range, using thermogravimetric and chemical titration analysis. The maximum oxygen deficiency of $LiMn_2O_{4-\delta}$ was found to be $\delta_{cr} = \sim 0.2$. For the samples obtained at 1023 K, as δ increased from 0, the tetragonal spinel phase appeared around $\delta = 0.07$, while only the cubic spinel phase was observed for the samples with $\delta \leq 0.07$. The dependence of δ on pO_2 was expressed as $\delta = \sim pO_2^{-(0.67 \pm 0.06)}$. In order to explain this relation, we employed a defect cluster model consisting of four Mn^{3+} ions and two oxygen vacancies. On the other hand, the sample with $\delta = 0.67$ was found to decompose to $LiMnO_2$ and Mn_3O_4. © 1997 Published by Elsevier Science S.A.

Keywords: Oxygen nonstoichiometry; Thermogravimetric analysis; Lithium manganese oxides; Spinel

1. Introduction

In order to search for a suitable cathode material for rechargeable lithium batteries, various kinds of ternary oxides, which contain a transition metal element and lithium, have been investigated eagerly during the past 15 years [1–3]. Among them, $LiMn_2O_4$ spinel is considered to be one of the most promising candidates due to a reversible intercalation of lithium ions [4]. Correctly speaking, lithium insertion into $Li_{1+x}Mn_2O_4$ induces a structural phase transition from a cubic to a tetragonal phases at $x = 0$ due to a cooperative Jahn–Teller distortion of Mn^{3+} ions [3]. Hence, the average valence of Mn ions in $Li_{1+x}Mn_2O_4$ plays a significant role to determine not only the cathode capacity but also the crystal structure.

Furthermore, according to recent reports [5–7], the composition of the $LiMn_2O_4$ sample annealed in a reducing atmosphere is represented as $LiMn_2O_{4-\delta}$. In order to balance the charge in $LiMn_2O_{4-\delta}$, the average valence of Mn ions should decrease in proportion to oxygen nonstoichiometry δ. As a result, δ is one of the essential factors to control the structural and electronic properties of $LiMn_2O_{4-\delta}$, as well as cathode performance of the lithium batteries. Here, we report δ of $LiMn_2O_{4-\delta}$ with respect to pO_2 and temperature and

discuss the mechanism for formation of oxygen defects using a defect cluster model.

2. Experimental

A powder sample of $LiMn_2O_4$ was synthesized by a solid-state reaction technique using reagent-grade Li_2CO_3 and MnO_2 powders. The $LiMn_2O_4$ powder of ~ 100 mg was placed in a platinum crucible; the crucible was suspended in a furnace tube by a platinum wire at temperatures between 873 and 1123 K for 24 h in an O_2/Ar gas mixture flow. In order to quench the sample to 273 K, the crucible was lowered onto glass wool, which was placed at the bottom of the tube, onto glass wool in a few seconds; the glass wool was placed at the bottom of the tube, and the bottom of the tube was immersed in ice-water. The oxygen nonstoichiometry, δ, was measured using a thermogravimetric technique. The absolute values of δ were determined by an induction coupled plasma analysis and a chemical titration analysis using $KMnO_4$. The measurement accuracy of δ was estimated to be ± 0.005.

3. Results

Fig. 1 shows the relationship between δ and $\log pO_2$ at temperatures between 873 and 1123 K for $LiMn_2O_{4-\delta}$. There
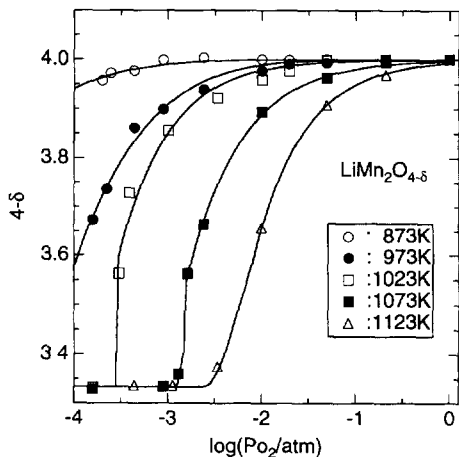
Fig. 1. The relationship between oxygen nonstoichiometry $4 - \delta$ and oxygen partial pressure log pO_2 for $LiMn_2O_{4-\delta}$ obtained at temperatures between 873 and 1123 K.
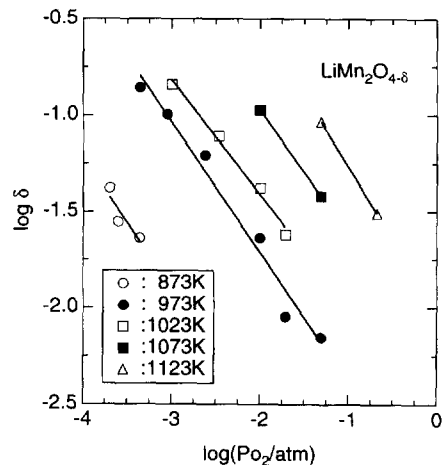

Fig. 2. The dependences of log δ–log pO_2 for $LiMn_2O_{4-\delta}$ obtained at temperatures between 873 and 1123 K.

were no marked differences between the data obtained on decreasing pO_2 and on increasing pO_2; thus, formation of oxygen deficiency in $LiMn_2O_4$ is found to be a reversible reaction with respect to pO_2. For the data obtained at 873 and 973 K, $4 - \delta$ decreased monotonically with lowering pO_2. On the other hand, for the data obtained at 1023 K, as pO_2 lowered, $4 - \delta$ decreased monotonically to $4 - \delta = \sim 3.6$, suddenly decreased from 3.6 to 3.33 at log $pO_2 = -3.6$, and then $4 - \delta$ leveled off to a constant value, $4 - \delta = 3.33$ in the pO_2 range below $10^{-3.6}$ atm. The log pO_2 versus $(4 - \delta)$ curves obtained at 1073 and 1123 K were similar to that obtained at 1023 K, though the sudden decreases in $4 - \delta$ were observed around log $pO_2 = -2.9$ at 1073 K and log $pO_2 = \sim -2.0$ at 1123 K, respectively. According to a powder X-ray diffraction (XRD) analysis, the samples with $4 - \delta > 3.85$ were assigned to be a single phase of a cubic spinel structure or to be a mixture of a cubic and a tetragonal spinel phases, while the samples with $3.33 < 4 - \delta \leq 3.75$ were a mixture of $LiMn_2O_{4-\delta}$, $LiMnO_2$ and Mn_3O_4. Therefore, the maximum oxygen deficiency was found to be $\delta_{cr} = \sim 0.2$. Furthermore, the sample with $4 - \delta = 3.33$ decomposed into $LiMnO_2$ and Mn_3O_4.

Fig. 2 shows the dependences of log δ–log pO_2 for the $LiMn_2O_{4-\delta}$ samples with $\delta \leq 0.20$ obtained at temperatures between 873 and 1123 K. Since five log δ–log pO_2 curves seem to be approximately parallel each other, it is considered that oxygen deficiency is formed through a same process. The average value of the slope of the five log δ–log pO_2 curves was estimated to be -0.67 ± 0.06.

4. Discussion

In order to explain the relationship between log δ–log pO_2, we employ a cluster model proposed for perovskites
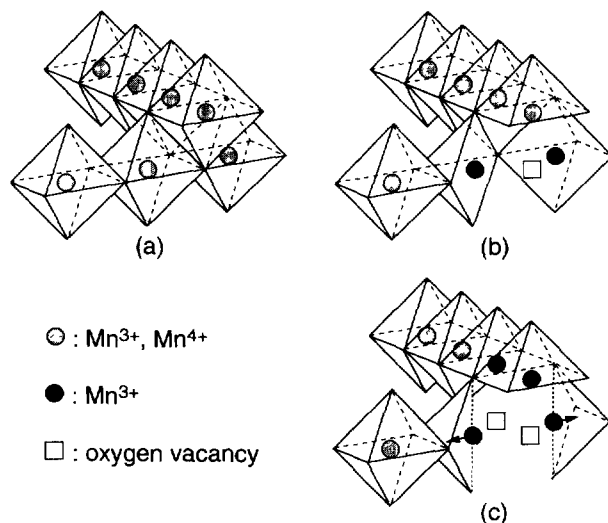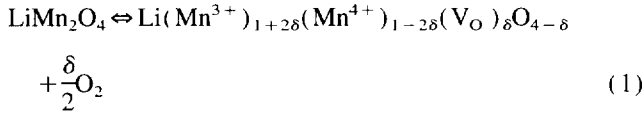

Fig. 3. (a) Spinel $LiMn_2O_4$ structure, only the MnO_6 octahedra are shown. (b) Simple cluster model (Model 2), two Mn^{3+} ions are bound to the oxygen vacancy. (c) More complicated cluster model (Model 3), four Mn^{3+} ions are bound to two oxygen vacancies.

$LaMnO_{3-\delta}$ and $LaCoO_{3-\delta}$ by Van Roosmalen and Cordfunke [8]. However, every oxygen ion of spinel $LiMn_2O_4$ has four nearest neighbors, i.e. three Mn ions and one Li ion. In addition, the connection between MnO_6 octahedra in spinel is characterized as edge-sharing, see Fig. 3(a), while that in perovskite as corner-sharing. Furthermore, we assume that only the valence of the Mn ions in $LiMn_2O_{4-\delta}$ alters caused by the formation of oxygen deficiency. Consequently, their cluster model could be modified, see Sections 4.1 to 4.3.
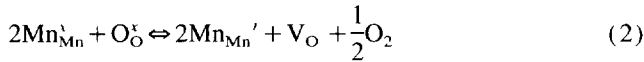
4.1. Point defect model

We assume that there is no interaction among oxygen defects and between oxygen defects and Mn ions; in other

words, both oxygen vacancies and Mn^{3+} ions are randomly distributed on the spinel lattice sites. We will abbreviate this model hereafter as Model 1. The equilibrium reaction for the loss of oxygen from $LiMn_2O_4$ by Model 1 can be expressed as
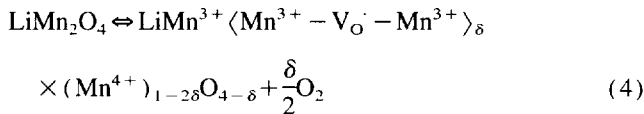
$$LiMn_2O_4 \Leftrightarrow Li(Mn^{3+})_{1+2\delta}(Mn^{4+})_{1-2\delta}(V_O)_\delta O_{4-\delta}$$
$$+ \frac{\delta}{2}O_2 \qquad (1)$$

or

$$2Mn^x_{Mn} + O^x_O \Leftrightarrow 2Mn_{Mn}{}' + V_O + \frac{1}{2}O_2 \qquad (2)$$

where Mn^x_{Mn} means Mn^{4+} on the Mn sites, Mn'_{Mn} Mn^{3+} in place of Mn^{4+}, V_O O^{2-} vacancy with $2+$ charge. The equilibrium constant for this reaction K_1 is given by
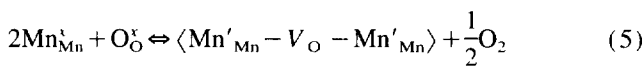
$$K_1 = \frac{[Mn_{Mn}{}']^2[V_O]pO_2^{1/2}}{[Mn^x_{Mn}]^2[O^x_O]} = \frac{4\delta^3 pO_2^{1/2}}{(1-2\delta)^2(4-\delta)} \qquad (3)$$

4.2. Simple cluster model

Assuming that there is an interaction between oxygen defects and Mn^{3+} ions, a defect cluster $\langle Mn^{3+}-V_O-Mn^{3+}\rangle$ may be formed to minimize an electrostatic repulsion, see Fig. 3(b). We will abbreviate this model hereafter as Model 2. For Model 2, the equilibrium reaction can be expressed as

$$LiMn_2O_4 \Leftrightarrow LiMn^{3+}\langle Mn^{3+} - V_O - Mn^{3+}\rangle_\delta$$
$$\times (Mn^{4+})_{1-2\delta}O_{4-\delta} + \frac{\delta}{2}O_2 \qquad (4)$$

or

$$2Mn^x_{Mn} + O^x_O \Leftrightarrow \langle Mn'_{Mn} - V_O - Mn'_{Mn}\rangle + \frac{1}{2}O_2 \qquad (5)$$

The equilibrium constant for this reaction K_2 is given by

$$K_2 = \frac{[\langle Mn'_{Mn} - V_O - Mn'_{Mn}\rangle]pO_2^{1/2}}{[Mn^x_{Mn}]^2[O^x_O]}$$
$$= \frac{\delta pO_2^{1/2}}{(1-2\delta)^2(4-\delta)} \qquad (6)$$

4.3. More complicated cluster model

If we assume a strong interaction between oxygen defects, a more complicated cluster is also available for the spinel lattice containing oxygen defects; that is, as seen in Fig. 3(c), a cluster which consists of four Mn^{3+} ions and two oxygen defects.
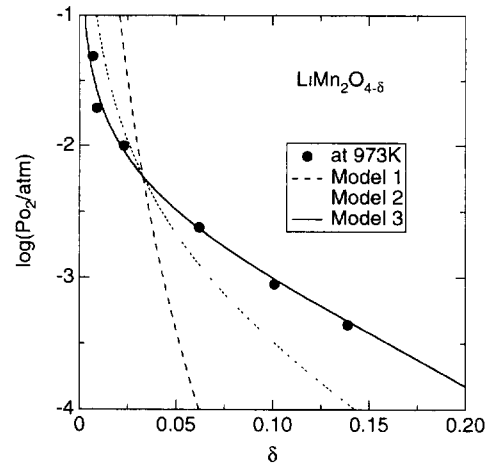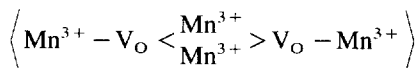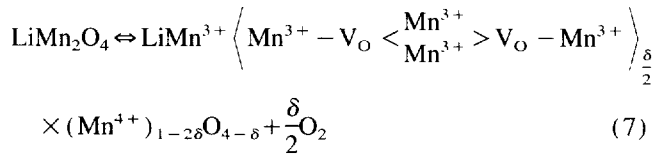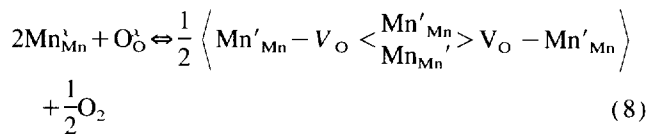
$$\left\langle Mn^{3+} - V_O < \frac{Mn^{3+}}{Mn^{3+}} > V_O - Mn^{3+}\right\rangle$$

Fig. 4. The dependences of $\log pO_2$ on δ: ($\bullet$) experimental data obtained at 973 K; (— — —) calculated dependence using Model 1; ($\cdots$) Model 2, and (———) Model 3.

We will call this model hereafter as Model 3. The equilibrium reaction can be expressed as

$$LiMn_2O_4 \Leftrightarrow LiMn^{3+}\left\langle Mn^{3+} - V_O < \frac{Mn^{3+}}{Mn^{3+}} > V_O - Mn^{3+}\right\rangle_{\frac{\delta}{2}}$$
$$\times (Mn^{4+})_{1-2\delta}O_{4-\delta} + \frac{\delta}{2}O_2 \qquad (7)$$

or

$$2Mn^x_{Mn} + O^x_O \Leftrightarrow \frac{1}{2}\left\langle Mn'_{Mn} - V_O < \frac{Mn'_{Mn}}{Mn'_{Mn}} > V_O - Mn'_{Mn}\right\rangle$$
$$+ \frac{1}{2}O_2 \qquad (8)$$

The equilibrium constant for this reaction K_3 is given by

$$K_3 = \frac{\left[\left\langle Mn'_{Mn} - V_O < \frac{Mn'_{Mn}}{Mn'_{Mn}} > V_O - Mn'_{Mn}\right\rangle\right]^{1/2}pO_2^{1/2}}{[Mn'_{Mn}]^2[O^x_O]}$$
$$= \frac{\delta^{1/2}pO_2^{1/2}}{(1-2\delta)^2(4-\delta)} \qquad (9)$$

Fig. 4 shows the dependences $\log pO_2-\delta$; the solid circles represent the experimental data obtained at 973 K, the broken line represents the calculated dependence using Model 1, the dotted line Model 2 and the solid line Model 3, respectively. The calculated result using Model 3 seems to fit in with the experimental data compared with those using other two models. Furthermore, the relationships between $\log pO_2-\delta$ at temperatures between 873 and 1123 K are shown in Fig. 5; the calculated relationships according to Model 3 are also plotted. Since the experimental data are in good agreement with the calculated relationships, the defect cluster is considered to be formed through a same process in the temperature range between 873 and 1123 K. Fig. 6 shows the temperature
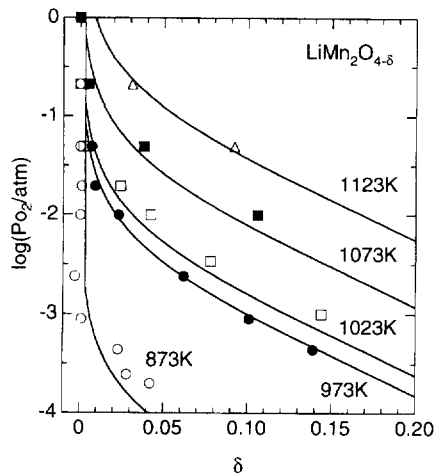
Fig. 5 The relationships between log pO_2 and δ obtained at temperatures between 873 and 1123 K, the solid lines represent the calculated relationships according to Model 3.
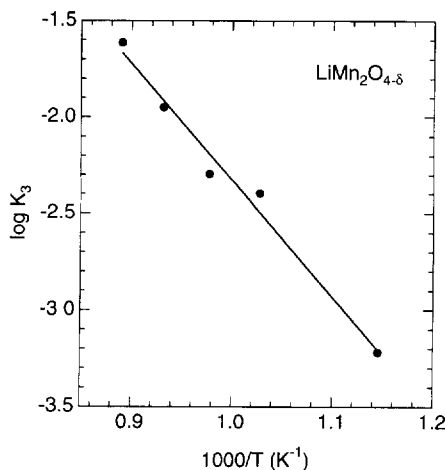

Fig 6 Temperature dependence of equilibrium constant K_3; K_3 was estimated by fitting the experimental data using Model 3.

dependence of the equilibrium constant K_3 estimated using Eq. (9) and the experimental data. Molar enthalpy ΔH_V^0 and entropy ΔS_V^0 of the formation of the defect cluster are given by

$$RT \ln K_3 = -\Delta H_V^0 + T\Delta S_V^0 \qquad (10)$$

On the basis of a linear fit (see Fig. 6), we obtain $\Delta H_V^0 = (116 \pm 9)$ kJ mol^{-1} and $\Delta S_V^0 = (31 \pm 4)$ J K^{-1} mol^{-1} in the 873 and 1123 K temperature range. These values are rather small compared with the values of the formation of the defect cluster, $\langle Mn^{2+}-V_O-Mn^{2+} \rangle$, in LaMnO$_{3-\delta}$ [9], i.e. $\Delta H_V^0 = (349 \pm 6)$ kJ mol^{-1} and $\Delta S_V^0 = (96.4 \pm 4.9)$ J K^{-1} mol^{-1}. This implies the possibility that the defect cluster in LiMn$_2$O$_{4-\delta}$ is more easily formed than in LaMnO$_{3-\delta}$.

Nevertheless, there is no evidence that such complicated cluster exists in LiMn$_2$O$_{4-\delta}$. Since such defect clusters give rise to a strong local distortion in the lattice, a structural analysis of LiMn$_2$O$_{4-\delta}$ would be useful to investigate the defect structure; therefore, the study of an X-ray absorption near-edge structure (XANES) on the Mn K-edge of LiMn$_2$O$_{4-\delta}$ is in progress. Furthermore, we ignored the role of Li$^+$ ions in the above discussion; this is because, to the authors' knowledge, there have been no data on the distribution of Li$^+$ ions and oxygen vacancies in LiMn$_2$O$_{4-\delta}$. In order to understand the effects of Li$^+$ ions on the defect structure, it is necessary to carry out a neutron diffraction analysis of LiMn$_2$O$_{4-\delta}$. In addition, there is a possibility that Mn^{2+} ions exist in LiMn$_2$O$_{4-\delta}$, because the average coordination number of the Mn ions in the defect cluster of Model 3 seems to be too small for Mn^{3+} ions. Thus, it is interesting to investigate magnetic properties of LiMn$_2$O$_{4-\delta}$ as a function of δ.

5. Summary

Using a thermogravimetric analysis and a chemical titration analysis, we investigated oxygen nonstoichiometry δ for a spinel LiMn$_2$O$_{4-\delta}$ sample as a function of oxygen partial pressure pO_2 in the 873 and 1123 K temperature range. The maximum oxygen deficiency of LiMn$_2$O$_{4-\delta}$ was found to be $\delta_{ci} = \sim 0.2$ and the dependence of δ on pO_2 was expressed as $\delta = \sim pO_2^{(-0.67 \pm 0.06)}$. In order to explain this relationship, we employed the following three defect cluster models: (i) a point defect model; (ii) a simple cluster model, in which two Mn^{3+} ions were bound to one oxygen vacancy, i.e. $\langle Mn^{3+}-V_O-Mn^{3+} \rangle$, and (iii) a more complicated cluster model in which four Mn^{3+} ions were bound to two oxygen vacancies, i.e.

$$\left\langle Mn^{3+} - V_O < \begin{matrix} Mn^{3+} \\ Mn^{3+} \end{matrix} > V_O - Mn^{3+} \right\rangle$$
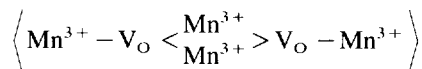
Making comparison with the experimental result, the Model 3 was considered to be suitable for LiMn$_2$O$_{4-\delta}$. Molar enthalpy ΔH_V^0 and entropy ΔS_V^0 of the formation for the cluster of the Model 3 were estimated to be $\Delta H_V^0 = (116 \pm 9)$ kJ mol^{-1} and $\Delta S_V^0 = (31 \pm 4)$ J K^{-1} mol^{-1}, respectively.

References

[1] J. Desilvestro and O. Haas, *J. Electrochem. Soc.*, *137* (1990) 5C–22C, and Refs. therein

[2] B. Scrosati, *J. Electrochem. Soc.*, *139* (1992) 2776–2781, and Refs. therein

[3] T. Ohzuku, in G. Pistoia (ed), *Lithium Batteries*, Elsevier Science, Amsterdam, 1994, pp. 239–280, and Refs. therein

[4] M.M. Thackeray, W.I.F. David, P.G. Bruce and J.B Goodenough, *Mater. Res. Bull., 18* (1983) 461–472.

[5] J.M. Tarascon, W.R. McKinnon, F. Coowar, T.N. Bowmer, G. Amatucci and D. Guyomard, *J. Electrochem. Soc., 141* (1994) 1421–1431.

[6] A Yamada, K. Miura, K. Hinokuma and M Tanaka, *J Electrochem. Soc, 142* (1995) 2149–2156.

[7] J Sugiyama, T. Atsumi, T. Hioki, S Noda and N Kamegashira, *J. Alloys Comp, 235* (1996) 163–169.

[8] J.A M. Van Roosmalen and H.P. Cordfunke, *J Solid State Chem., 93* (1991) 212–219.

[9] J.A M. Van Roosmalen and H.P. Cordfunke, *J. Solid State Chem., 110* (1994) 113–117.